Short-time dynamics of colloidal particles confined between two walls

Jesús Santana-Solano and José Luis Arauz-Lara
Instituto de Física "Manuel Sandoval Vallarta," Universidad Autónoma de San Luis Potosí, Alvaro Obregón 64, 78000 San Luis Potosí, San Luis Potosí, Mexico
(Received 7 June 2001; published 17 January 2002)

The short-time dynamics of colloidal particles in a quasi-two-dimensional geometry is studied by digital video microscopy. The particles (polystyrene spheres) are suspended in water and confined between two parallel glass plates, forming an effective two-dimensional system. The (effective) two-dimensional van Hove function $G(r,t)$ and its self and distinct part are measured with a time resolution of 1/30 s. We found that the general behavior of these time-correlation functions (and their Fourier transforms) is quite similar to that of their three-dimensional counterparts. The effects of the strong hydrodynamic coupling of the particles motion to the walls and that due to the hydrodynamic interactions between particles are contained in the (effective) hydrodynamic function $H(k)$ obtained from the initial slope of $F(k,t)$ [the Fourier transform of $G(r,t)$]. We found that $H(k)$, as a function of the wave vector k and particle concentration, exhibits a similar qualitative behavior to the hydrodynamic function in homogeneous three-dimensional suspensions of hard spheres. We also found in our systems that the particle fluctuations relax only by self-diffusion for wave vectors where the static structure factor $S(k)=1$. This result is important for measurements of self-diffusion dynamics in three-dimensional systems by light scattering techniques.

DOI: 10.1103/PhysRevE.65.021406 PACS number(s): 82.70.Dd, 05.40.−a

I. INTRODUCTION

The dynamics of confined colloidal particles is a subject of wide interest and of great scientific and technological relevance, which is increasingly attracting the attention of many researchers [1–10]. The recent interest is partly due to the availability of direct imaging techniques that allow one to study the particles dynamics in real space in great detail. Colloidal dynamics has been extensively studied for more than two decades in the case of homogeneous three-dimensional (3D) suspensions (of charged and hard spheres). There, theory, experiments, and computer simulations have led to an understanding of many aspects of the dynamic processes in the bulk [11–17]. However, the description of those processes when they occur under confinement, is still in a far less developed stage owing to the considerable additional complexity introduced by the confining conditions. In this case, the dynamic properties are not only determined by the direct (DI) and hydrodynamic (HI) interparticle interactions, the motion of the particles is also coupled to the confining walls by DI and HI. This makes the description considerably more complicated than in 3D. The more striking effects are, perhaps, those arising from strong hydrodynamic coupling of the particles with the walls. For instance, the translation (and rotation) friction coefficient of an isolated particle (a scalar quantity in the bulk) moving close to a single plane wall becomes a tensor, with its parallel and perpendicular components diverging as the particle approaches the wall's surface [18,19]. The presence of a second (parallel) wall complicates significantly the description. In this case the contributions from an infinite number of reflections between the two walls of the hydrodynamic flux of the suspending fluid have to be incorporated [20]. For an isolated pair of particles close to a single wall, a detailed study of the relative particles' motion has shown the strong effect of the hydrodynamic interactions with the wall [7,8]. These examples illustrate the determinant role of the long-ranged hydrodynamic interactions as well as the complexity involved in their description even in simple cases. Thus, the interesting and challenging problem at hand is the study of the dynamics of a finite number of colloidal particles, either close to a single wall or confined between two of them, where particle-particle and particle-wall(s) interactions (direct and hydrodynamic) are present.

The aim of the present work is, precisely, the study of the effects of confinement on the dynamic processes in colloidal suspensions at finite concentrations, and in particular the effects of the hydrodynamic interactions. We consider the specific case of quasi-two-dimensional systems, i.e., colloidal suspensions highly confined between two parallel walls. Here we are mainly interested in the effects of HI both between particles and between particles and the walls. Thus, we study concentrated systems where such effects are strong, but we focus only on the short-time regime, where the effects of the HI can be decoupled from those of the DI. In a recent work [10] we addressed this problem and presented measurements of effective two-dimensional quantities describing the effects of the HI. Here we study essentially the same problem, but we provide a more extensive account of the experimental details and an extended presentation of the physical quantities describing short-time dynamics, those measured in our experiment. We confine colloidal particles (diameter $\sigma = 2.05\ \mu$m, suspended in water) between two parallel plates separated a distance ($h = 2.92\ \mu$m) comparable to the particles size. The presence of the plates forces the particles to form a single layer in the midplane parallel to the walls. Under these conditions, the particles motion occurs (mainly) along that plane since the motion in the perpendicular direction is severely restricted. We use optical microscopy to observe and record the in-plane dynamics of the particles in real space. Thus, in our experiment we define and measure experimentally accessible quantities as if the systems were strictly two-dimensional (2D). However, although the motion

of the colloidal particles is essentially two dimensional, the motion of the suspending fluid is not restricted to 2D. Thus the measured quantities, defined analogously to those describing the dynamic properties in bulk suspensions, are in reality effective 2D quantities containing the effects of the confinement that we want to study. The formal derivation of a theory describing the dynamic properties of our experimental system would have to incorporate a number of rather complex effects, such as the (direct and hydrodynamic) interactions of the particles, not only among themselves, but also with the confining walls. Thus, its derivation will be considerably more complicated than in 3D. Instead of pursuing such derivation here, we adopted a practical approach by defining and measuring effective 2D quantities as discussed in the following sections. Interestingly, we find that the properties thus defined and measured exhibit a qualitative behavior strikingly similar to their 3D counterparts. This indicates that, in spite of all the complexity involved, the description of the dynamics of colloidal particles in quasi-two-dimensional geometries can be cast in a fashion formally no more complicated than in the case of 3D bulk suspensions. Clearly, this observation should serve as an important guideline for the future development of the theory of the dynamics of confined suspensions. A computer simulation study, of the HI effects on the dynamic properties of colloidal particles confined in a similar geometry as in our experiment, has been reported by Pesché and Nägele [9]. In that work, the authors use Stokesian dynamics to account for the HI, particle-particle, and particle wall, in systems of charged and neutral particles. Although that work is similar to ours, the authors study different systems and conditions. Thus, a direct quantitative comparison between their computer simulation results and our experimental data is (unfortunately) not possible at this stage. In Sec. II we give a more detailed account of the experimental methods. In Sec. III we present and discuss our results, and in Sec. IV we present our conclusions.

II. METHODS

A. System preparation

Aqueous suspensions of polystyrene spheres of diameter $\sigma = 2.05 \pm 3\%$ μm and $\sigma_2 = 2.92 \pm 3\%$ μm (Duke Scientific) were extensively dialyzed (dialysis bags of 50 000 molecular weight cutoff) against nanopure water to eliminate the surfactants in the original batches. In a clean atmosphere of nitrogen gas, the suspension of small particles is mixed with a small amount of large particles. A little volume of the mixture
(≈ 1 μl), is confined between two carefully cleaned glass plates (a slide and a cover slip), which are uniformly pressed one against the other until the separation h between the plates coincides with σ_2. As a result, the large particles are fixed in a disordered configuration across the sample, serving as spacers between the plates. The system is then sealed with epoxy resin (Epo-Tek 302), and the species of small mobile particles is allowed to equilibrate in this confined geometry for a few days at room temperature ($27.7 \pm 0.1\,^{\circ}$C). Under these conditions, the motion along the direction z, perpendicular to the plates, is almost suppressed, and the main motion of the particles is along the plane (x,y) parallel to the walls. Thus, the mobile species constitute an effective two-dimensional colloidal suspension, homogeneous along the plane of motion. Systems with different concentrations of mobile particles were prepared following this procedure and they remained stable for several months. Figure 1 shows an image of area $a = 76 \times 56$ μm^2 of a sample with mobile particles area fraction $\phi_a \equiv \pi n^*/4 = 0.38$, $n^* \equiv n\sigma^2$ is the reduced concentration, and n is the average number of particles in the area a. The image was taken using an optical microscope with a $40\times$ objective. In this figure only the mobile particles can be seen, but fixed spacer particles are scattered around the area of observation. We obtained identical results for the physical quantities of interest from measurements at different sites of the system.

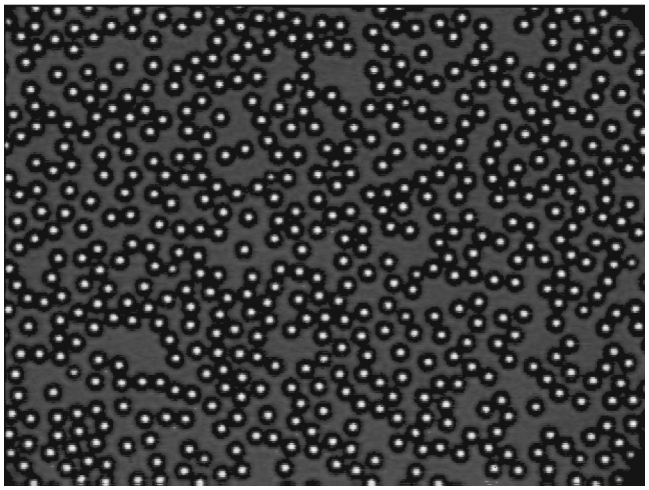

FIG. 1. Top view of a quasi-two-dimensional colloidal suspension of area fraction $\phi_a = 0.38$. The image is 76×56 μm^2 and the particles' diameter $\sigma = 2.05$ μm.

B. Digital video microscopy

The systems are observed in real space using an optical microscope with a $40\times$ objective. The motion of the particles is recorded using a charge-coupled device (CCD) camera coupled to a videotape recorder. Images are digitized (see Fig. 1) using a frame grabber with a resolution of 640 $\times$480 pixels. With our setup we measure $\sigma = 16.8$ pixels. The position (i.e., the x and y coordinates) of every particle in the field of view is determined from the digitized images using the method devised by Crocker and Grier [21], which allows us to locate the spheres centers with a precision of 1/5 pixel ($\sim 0.01\sigma$). The particles motion in our system is quite slow; they move on average only a small fraction of σ between frames. Thus, their 2D trajectories can be easily reconstructed, with a time resolution of 1/30 s, from their positions at consecutive frames. From the trajectories, we obtain various effective 2D physical quantities describing self-dynamics and collective dynamics, as we explain below. All the results presented here were obtained from the analysis of at least 10^4 video frames in runs of 120 consecutive frames. Figure 2 shows the trajectories of the particles in the system shown in Fig. 1, as obtained from one run.

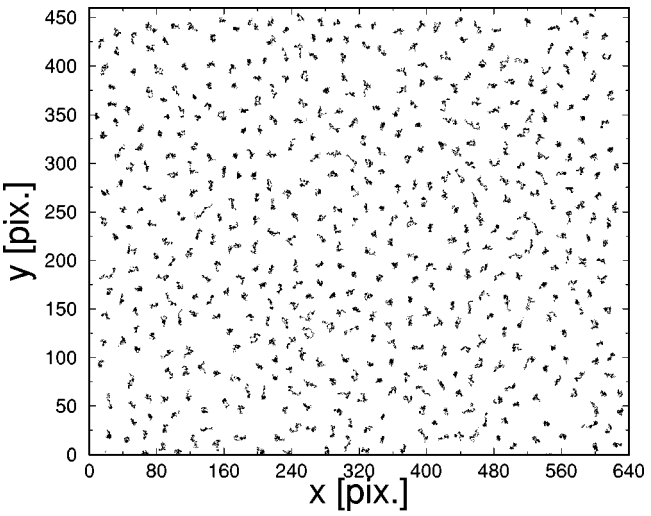

FIG. 2. Trajectories of the particles in Fig. 1 obtained from 120 consecutive video frames.

III. RESULTS

A. Static structure

Before discussing the dynamic properties, let us present measurements of an important equilibrium property of the system which depends only on the direct interactions, namely, the static structure. In real space it is characterized by the radial distribution function; the conditional probability of finding a particle a distance r far away from a central particle. In our quasi-two-dimensional systems we measure the in-plane radial distribution function $g(r)$, with r being the projection of the distance between particles' centers along the plane (x,y). Figure 3 shows the measured $g(r)$ for four different particle concentrations (dots with dashed line). As it is seen here, the structure increases as the concentration increases. For the less concentrated system studied here, $\phi_a = 0.23$, $g(r)$ shows clearly one maximum, and the presence of a minimum and a second maximum is only insinuated. As ϕ_a increases, the height of the first peak also increases and subsequent maxima and minima are developed. The position of the first peak is close to contact ($\sim 1.1\sigma$), meaning that the effective direct interparticle interaction is short ranged. One can also see in this figure that the shape of $g(r)$ resembles that of a radial distribution function of a system of hard disks. In order to check this observation more quantitatively, we run a computer simulation using the Monte Carlo (MC) algorithm for strictly two-dimensional systems of hard disks of diameter σ at the same area fractions of the experimental systems. As one can see here, the MC $g(r)$ (solid lines in Fig. 3) follow closely the experimental results with small deviations. Thus, according to this comparison, the dominant component of the interparticle direct interaction is the excluded volume interaction. However, the facts that the first peak of the experimental $g(r)$ is not exactly at contact and small but consistent discrepancies are observed between the simulated and the experimental radial distribution functions are indications of the existence of an additional (small) component in the effective particle-particle interacting potential. This is an interesting and important matter in its own right, but is not within the main subject of the present work. We will provide a more detailed discussion of these and other complementary experiments in a separated report.

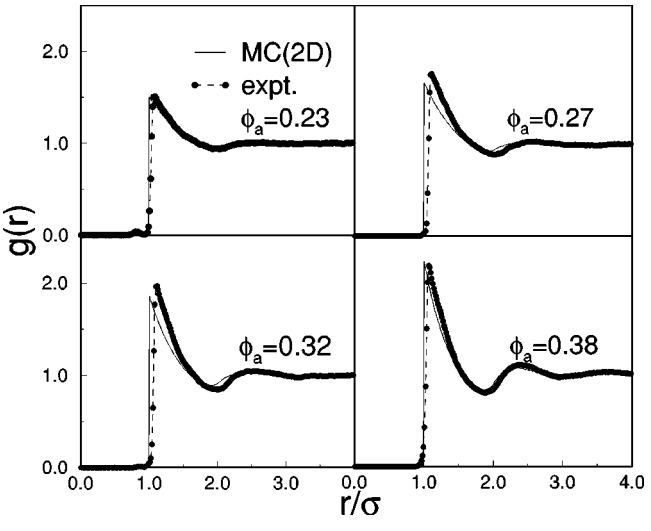

FIG. 3. Measured in-plane radial distribution function $g(r)$ of quasi-two-dimensional colloidal suspensions for four different area fractions (dots with dashed line). The solid lines are the radial distribution functions of strictly 2D systems of hard disks at the same area fractions obtained by Monte Carlo computer simulations.

B. In-plane self-diffusion

The in-plane Brownian motion of individual particles, also referred to as self-diffusion, can be described in terms of a simple quantity, namely, the particle's mean squared displacement $W(t)$ given by

$$W(t) = \frac{1}{4}\langle [\Delta \mathbf{r}(t)]^2 \rangle, \tag{3.1}$$

where $\Delta \mathbf{r}(t) = \mathbf{r}(t) - \mathbf{r}(0)$ is the particle's in-plane displacement at time t, and the angular brackets represent an equilibrium ensemble average. However, a more general quantity describing self-diffusion is the normalized probability distribution function $P(\Delta \mathbf{r},t)$ of single particle displacements $\Delta \mathbf{r}$ at time t, with $W(t)$ being only its second moment, i.e., $W(t) = \frac{1}{4}\int d\mathbf{r} (\Delta \mathbf{r})^2 P(\Delta \mathbf{r},t)$. These quantities, $P(\Delta \mathbf{r},t)$ and $W(t)$, are determined in our experiment directly from the particles trajectories. For homogeneous and isotropic systems in thermal equilibrium it should happen that $P(\Delta x,t) = P(\Delta y,t)$, with $P(\Delta x,t)$ and $P(\Delta y,t)$ being the normalized probability distribution functions of displacements along the directions x and y at time t, respectively, and $P(\Delta \mathbf{r},t) = P(\Delta x,t) P(\Delta y,t)$, with $|\Delta \mathbf{r}|^2 = \Delta x^2 + \Delta y^2$. In Fig. 4 we compare results for $P(\Delta x,t)$ (open symbols) and $P(\Delta y,t)$ (closed symbols) at different times, only for the system with $\phi_a = 0.38$ (the results for other area fractions are similar). This figure shows that in the quasi-two-dimensional systems studied here the equality $P(\Delta x,t) = P(\Delta y,t)$ holds, i.e., the motion of the particles along the direction x is indeed independent and equivalent to the motion in the direction y.

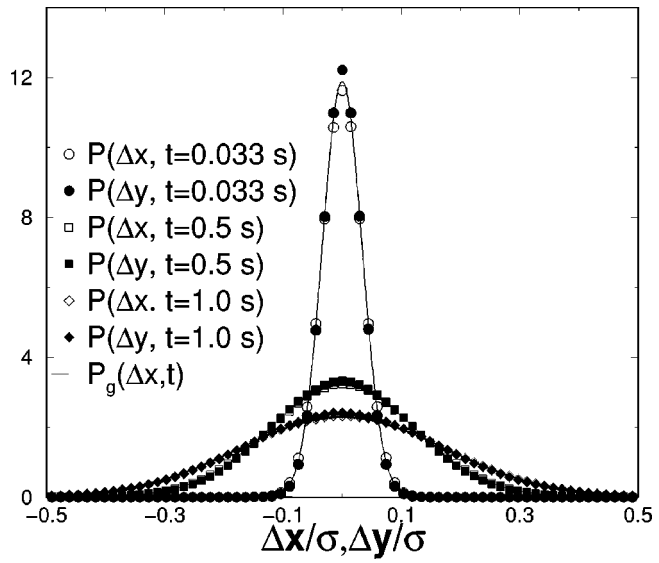

FIG. 4. Probability distribution functions of single particle displacements in the directions x and y for different times (symbols). Here one can see that the motion of the particles along the perpendicular directions is symmetric, independent, and equivalent. For comparison, we show the Gaussian functions with zero mean value and dispersion $\sqrt{\langle \Delta x^2(t)\rangle}$ (solid lines). In this system $\phi_a=0.38$, but similar results are obtained for other area fractions.

This indicates that the systems are homogeneous and isotropic along the (x,y) plane. Then, we can write $2W(t)=\langle[\Delta x(t)]^2\rangle=\langle[\Delta y(t)]^2\rangle$. Thus, we can describe the self-diffusion properties using only either $P(\Delta x,t)$ or $P(\Delta y,t)$. In this figure one can see that the functions $P(\Delta x,t)$ are symmetric, centered around $\Delta x=0$. Initially they are very narrow, and then they spread out as time increases due to self-diffusion of the particles. In isotropic systems of noninteracting particles the $P(\Delta x,t)$ are Gaussian functions with $\langle \Delta x\rangle=0$ and dispersion $\sqrt{\langle \Delta x^2(t)\rangle}$ [22]. For 3D colloidal suspensions at finite concentration, the corrections to the Gaussian form introduced by the interactions between the particles are negligible and $P(\Delta x,t)$ are very well approximated by Gaussian functions [23]. In the case of confined particles, one can ask whether the in-plane particles displacements are also random variables with Gaussian distributions, or the effects of the walls change the qualitative behavior of the individual motion of the particles. Thus, one could check how well the experimental $P(\Delta x,t)$ in Fig. 4 fit to Gaussian functions. We proceed here as we did in previous papers [3,10]. We compare the measured $P(\Delta x,t)$ with normalized Gaussian functions $P_g(\Delta x,t)$ having zero mean value and dispersion $\sqrt{2W(t)}$, i.e.,

$$P_g(\Delta x,t)=\frac{1}{\sqrt{4\pi W(t)}}\exp\left[-\frac{\Delta x^2}{4W(t)}\right]. \qquad (3.2)$$

Figure 4 shows also the functions $P_g(\Delta x,t)$ (solid lines), constructed using the measured mean squared displacement $W(t)$. As one can see here, the measured $P(\Delta x,t)$ coincides with the Gaussian distribution functions in a wide range of times (similar results are obtained for other concentrations).

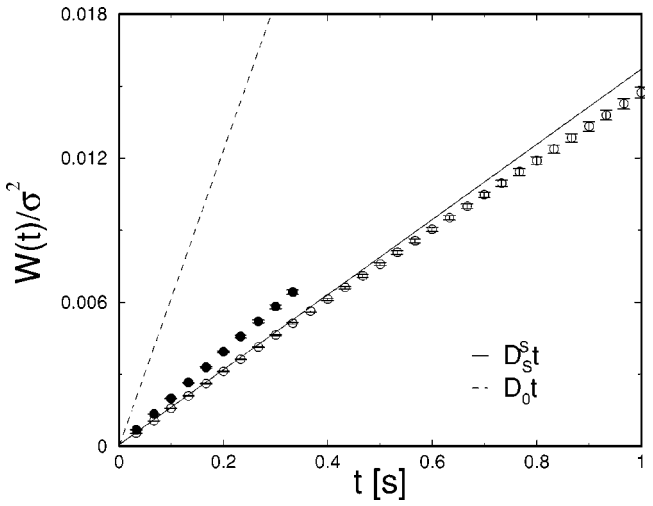

FIG. 5. Effective 2D mean squared displacement $W(t)$. Close ($\phi_a=2.3\times10^{-3}$) and open ($\phi_a=0.38$) circles are experimental data from video microscopy. The solid line is the initial linear behavior of $W(t)$ in the system with $\phi_a=0.38$, and the dashed line corresponds to free diffusion in 3D.

Thus, the individual lateral motion of the particles in our systems is essentially a Gaussian random process characterized only by its first two moments $\langle \Delta x(t)\rangle(=0)$ and $\langle[\Delta x(t)]^2\rangle[=2W(t)]$.

Figure 5 shows the measured $W(t)$ only for two illustrative cases, a highly dilute system ($\phi_a\sim2.3\times10^{-3}$) and the most concentrated system studied here ($\phi_a=0.38$). In the dilute system (closed circles), the effects of the interparticle interactions, direct and hydrodynamic, are negligible and $W(t)$ contains only the effects of the particle-walls hydrodynamic interactions. The effect of the direct interaction between the particles and the walls is the particles confinement. For this concentration, $W(t)$ is shown only for short times since reliable values of $W(t)$ at longer times requires the analysis of a considerable large amount of data. The dashed line in Fig. 5 is $W(t)=D_0t$, corresponding to free diffusion of the same particles in 3D, with $D_0=kT/3\pi\eta\sigma$ being the free diffusion coefficient. Comparison of the initial slope of $W(t)$ in the dilute system $D_s=8.28\times10^{-10}$ cm^2/s, with $D_0=2.59\times10^{-9}$ cm^2/s, shows that the hydrodynamic coupling of the particles with the walls has a strong effect already on the motion of isolated particles (D_s is only about 30% of D_0). At finite concentrations, in addition to the effects from the walls, the individual motion of the particles is also affected by the interparticle interactions, leading to a further reduction of the particles mobility, i.e., to lower values for $W(t)$ (open circles). In the bulk of homogeneous 3D systems, the mean squared displacement increases linearly with time at short times [i.e., $W(t)=D_s^st$] and it bends down at later times due to the effect of the direct interparticle interactions. The quantity $D_s^s\equiv\lim_{t\to0}W(t)/t$ is referred to as the short-time self-diffusion coefficient and its value decreases (from $D_s^s=D_0$ at infinite dilution) as the particle concentration increases due to the interparticle hydrodynamic interactions. The same features are observed in the quasi-two-dimensional systems. The solid line in Fig. 5 is a straight

line with its slope (D_s^S) determined by a linear regression using only the five initial experimental data points (0.166 s) of $W(t)$. As it is seen here, the linear regime spans up to about 0.5 s. For times $t>0.5$ s, $W(t)$ deviates from the linear behavior due to the direct interactions between neighboring particles. Thus, at finite particle concentrations, the initial slope D_s^S contains the effects of both the particle-particle and particle-walls hydrodynamic interactions. As it is seen here, the strongest effect comes from the hydrodynamic interactions with the walls since the difference between D_s^S and D_s is smaller than the difference between D_s and D_0.

C. In-plane collective dynamics: real space

In this section we present results for the in-plane collective dynamics. As mention above, we shall be mainly interested in studying the effects of the hydrodynamic interactions. Thus, we focus on the short-time regime where those effects can be decoupled from the effects of the direct interactions. The general quantity measured in our experiment is the time correlation function $G(r,t)$ of the 2D (in-plane) local particles concentration $n(\mathbf{r},t)$ at the (in-plane) position $\mathbf{r}$ and time t, i.e., $G(r,t)\equiv(1/N)\langle n(\mathbf{r}',t=0)n(\mathbf{r}'',t)\rangle$ with $r\equiv|\mathbf{r}''-\mathbf{r}'|$, and the angular brackets representing an equilibrium ensemble average. The local concentration is written as $n(\mathbf{r},t)=\Sigma_{j=1}^{N}\delta(\mathbf{r}-\mathbf{r}_j(t))$, with N being the number of particles in the system and $\mathbf{r}_j(t)$ the (in-plane) position of the j-particle at time t. Thus,

$$G(r,t)=\left\langle \sum_{j,l=1}^{N} \delta(\mathbf{r}-\mathbf{r}_j(t)+\mathbf{r}_l(0)) \right\rangle. \tag{3.3}$$

The correlation function $G(r,t)$, which describes the collective motion of the particles, can be split into two terms, the self-part and the distinct part, $G_s(r,t)$ and $G_d(r,t)$, respectively. The former containing the terms $j=l$ and the latter the terms $j\neq l$, i.e.,

$$G(r,t)=G_s(r,t)+G_d(r,t), \tag{3.4}$$

with

$$G_s(r,t)=\langle \delta(\mathbf{r}-\mathbf{r}_1(t)+\mathbf{r}_1(0))\rangle \tag{3.5}$$

and

$$G_d(r,t)=\frac{1}{N}\left\langle \sum_{j\neq l}^{N} \delta(\mathbf{r}-\mathbf{r}_j(t)+\mathbf{r}_l(0)) \right\rangle. \tag{3.6}$$

The quantity $G_s(r,t)$ describes the process of self-diffusion, i.e., the self-correlation of individual particles, and $G_d(r,t)$ describes the time correlation between different particles. These correlation functions, $G(r,t)$ and their self-part and distinct parts, are defined and measured in our experiment as if the systems were 2D. However, one should keep in mind that in reality they are effective two-dimensional quantities containing the effects of the confinement on the dynamic processes of the colloidal particles. We will refer here to $G(r,t)$ as the effective 2D van Hove function since the definition given above [Eq. (3.3)] coincides with the formal expression for the van Hove function for strictly 2D or 3D systems [where $\mathbf{r}$ and $\mathbf{r}_j(t)$ are 2D or 3D vectors, respectively]. It should be clear, however, that Eq. (3.3) is not the expression for the actual van Hove function for quasi-two-dimensional systems. The derivation of such an expression, certainly more complex than in 2D or 3D due to the presence of the confining walls, is not pursued here. Instead, we discuss the dynamic properties of the confined colloidal particles in terms of the effective 2D quantities introduced above and other quantities defined below.

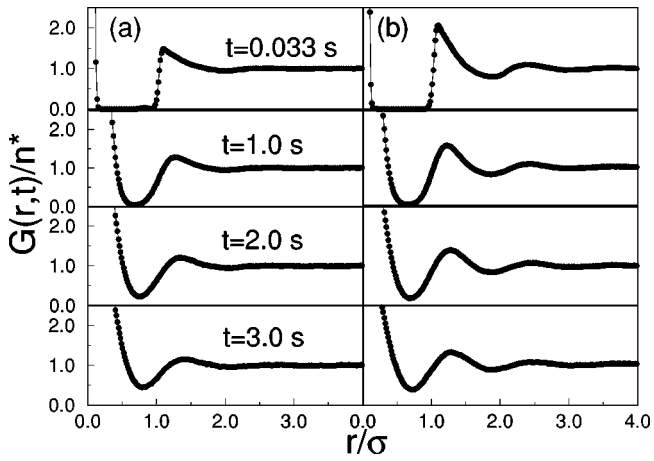

FIG. 6. Measured effective two-dimensional van Hove function $G(r,t)/n^*$ vs r/σ, at different times, for quasi-two-dimensional colloidal suspensions with (a) $\phi_a=0.23$ and (b) 0.38.

Figure 6 shows the measured effective two-dimensional van Hove function $G(r,t)$ for the systems with (a) $\phi_a=0.23$ and (b) 0.38. One can see here the contributions of the self-correlation and distinct-correlation functions to the total correlation function $G(r,t)$ at different times. For times $t<1$ s, both components are clearly distinguishable from each other, and at later times they merge together combining their relative contributions to $G(r,t)$. At time $t=0$, the self-part is a peaked function at $r=0$ (data not shown), i.e., $G_s(r,0)=\delta(r)$ [see Eq. (3.5)], and $G_d(r,0)=n^*g(r)$, with $g(r)$ being the in-plane radial distribution function. At times $t>0$, $G_s(r,t)$ spreads out, due to self-diffusion, following a Gaussian function with dispersion $\sqrt{2W(t)}$ as shown in Fig. 7, while the initial structure of the distinct part smears down due to the loss of interparticle correlation as time evolves. In fact, for very long times the dynamics of the particles is completely uncorrelated and the distinct part is a constant, i.e., $G_d(r,t)\to n^*$ as $t\to\infty$. Of particular interest is the time at which the contributions of $G_s(r,t)$ and $G_d(r,t)$ start to overlap. This time provides a quantitative way to define the time span of the short-time regime. In the set of (concentrated) systems studied here, the merging time is between 0.5 and 1 s.

D. In-plane short-time collective dynamics: reciprocal space

The dynamics of colloidal particles in 3D suspensions is usually studied in terms of the dynamic structure factor $F(k,t)$, which is the quantity measured in dynamic light scattering experiments. $F(k,t)$ is the Fourier transform of the

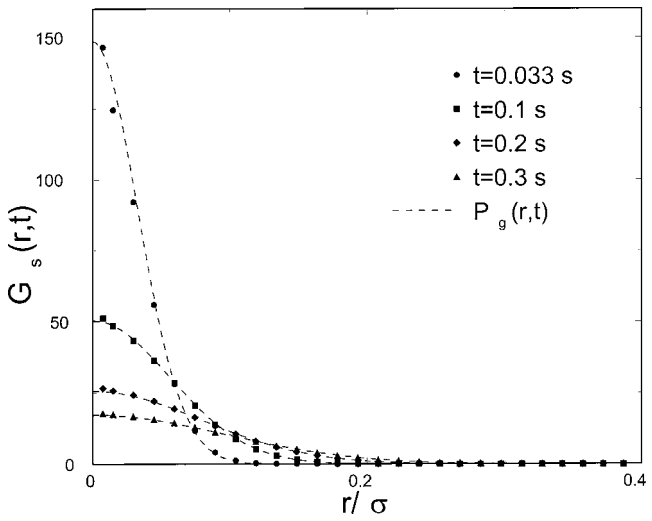

FIG. 7. Measured $G_s(r,t)$ vs r (symbols) compared with normalized Gaussian functions $P_g(r,t)$ (dashed lines) of width $\sqrt{2W(t)}$. In this system $\phi_a=0.38$.

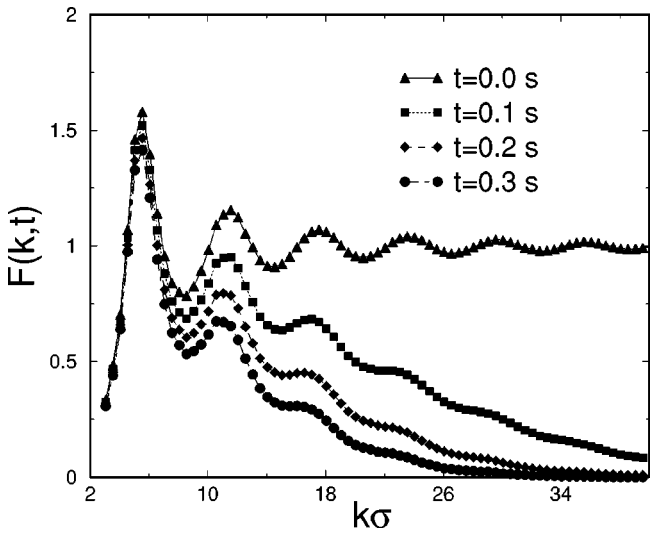

FIG. 8. Effective dynamic structure factor $F(k,t)$ vs k at different times. $F(k,t)$ is a decaying function of time, and the decay rate is increasingly faster for larger values of the wave vector.

3D van Hove function, i.e., it is the time correlation function of the fluctuations of the local particle concentration of wavelength $\lambda=2\pi/k$. Thus, the van Hove function and the dynamic structure factor describe the structural properties of colloidal suspensions in the real and in the reciprocal space, respectively. At short times, the correlation function $F(k,t)$ decays as [11,13]

$$F(k,t)=S(k)\exp[-k^2D_c^S(k)t], \tag{3.7}$$

where $S(k)=F(k,t=0)$ is the static structure factor and $D_c^S(k)$ is the short-time collective diffusion coefficient. Thus, the initial relaxation of thermal fluctuations in the local particle concentration is exponential, with a wavelength-dependent time constant. A very important property of $D_c^S(k)$ is that it can be written as the ratio of two quantities; one $[H(k)]$ describing the effects of the hydrodynamic interactions, and the other $[S(k)]$ being an equilibrium property that depends on the direct interactions, i.e., $D_c^S(k)=H(k)/S(k)$. Thus, the initial decay of $F(k,t)$ measures the effects of the HI. The function $H(k)$, referred to as the hydrodynamic function, is expressed as an ensemble average of the diffusion tensors $D_{lj}(\mathbf{r}^N)$, i.e.,

$$H(k)=\langle 1/N\Sigma_{l,j=1}^{N}\hat{\mathbf{k}}\cdot\mathbf{D}_{lj}(\mathbf{r}^N)\cdot\hat{\mathbf{k}}\exp(i\mathbf{k}\cdot[\mathbf{r}_l-\mathbf{r}_j])\rangle.$$

This quantity has interesting general properties. The self-part, $H_s=\langle\hat{\mathbf{k}}\cdot\mathbf{D}_{11}(\mathbf{r}^N)\cdot\hat{\mathbf{k}}\rangle$, is independent of k and quantifies the HI effects on single particle motion. H_s is the short-time diffusion coefficient given by the initial slope of the (3D) mean squared displacement $W(t)\equiv\langle[\Delta\mathbf{r}(t)]^2\rangle/6$, i.e., $H_s\equiv D_s^s=\lim_{t\to 0}W(t)/t$. Here, $t\to 0$ means the limit of short times within the diffusive time regime. The distinct part $H_d(k)$ of $H(k)$ (the terms $l\neq j$) describes the hydrodynamic coupling between particles l and j. This quantity is the ensemble average of a phase factor which oscillates very rapidly at large values of k. Thus, $H_d(k)\to 0$ and $H(k)\to D_s^s$ in the large wave-vector limit.

Thus, an important advantage of describing the dynamic properties of 3D systems in the reciprocal space is that, at short times, the HI and DI effects can be decoupled, with the former being measured by the initial slope of the dynamic structure factor. In our case the reciprocal space description of the dynamic properties is provided in terms of the (effective) 2D dynamic structure factor $F(k,t)$, defined here as the Fourier transform of the measured $G(r,t)$. Although $F(k,t)$ defined in this way is not, strictly speaking, the actual dynamic structure factor of our systems (for which a formal expression has yet to be derived), it should be clear that this quantity describes the dynamic processes in the Fourier space as far as $G(r,t)$ provides the appropriate description in the real space. $F(k,t)$ can also be written as the sum of two terms,

$$F(k,t)=F_s(k,t)+F_d(k,t), \tag{3.8}$$

with $F_s(k,t)$ and $F_d(k,t)$ being the Fourier transforms of $G_s(r,t)$ and $G_d(r,t)$, respectively. Since both components of $G(r,t)$ can be determined independently through the particles trajectories, then both components of $F(k,t)$ can also be determined independently. Figure 7 shows the self-part of $G(r,t)$ vs r at short times (symbols) for the system with $\phi_a=0.38$. As one can see here, it is a very narrow function of r and we have only few experimental data points defining this function. Thus, the determination of $F_s(k,t)$ from a direct Fourier transformation of the experimental data might be somewhat inaccurate. Figure 7 shows also a comparison of the measured $G_s(r,t)$ with Gaussian functions $P_g(r,t)$ (dashed lines), constructed from the measured $W(t)$. As one can see here, the experimental data are very well represented by $P_g(r,t)$. Thus, in order to avoid inaccuracies in the determination of $F(k,t)$, we proceeded in the following way for

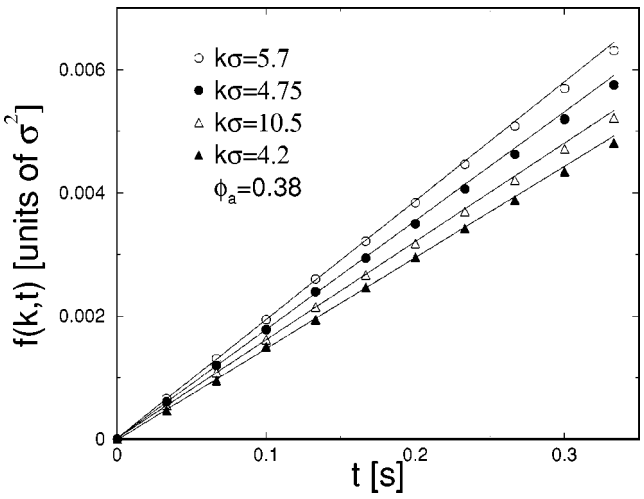

FIG. 9. $f(k,t)$ vs t (symbols) for various values of k. The initial slope (lines) defines the effective 2D hydrodynamic function $H(k)$.

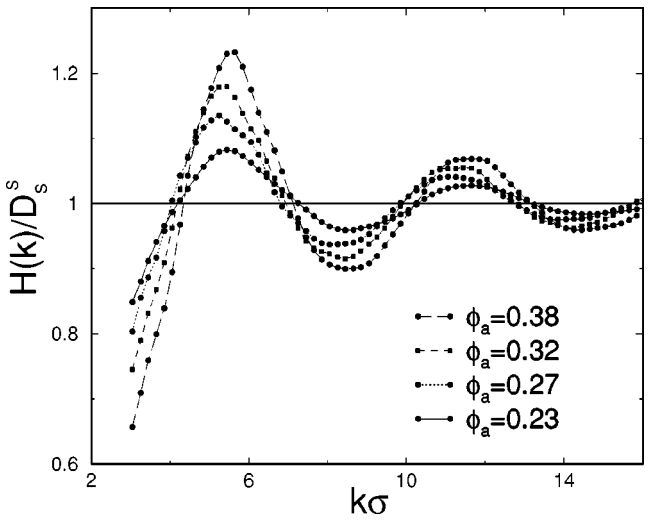

FIG. 10. Effective 2D hydrodynamic function, normalized with the 2D short-time self-diffusion coefficient, for various concentrated systems.

short times ($t<0.5$ s). The distinct part $F_d(k,t)$ is obtained by Fourier transforming the measured $G_d(r,t)$, and for $F_s(k,t)$ we use the Fourier transform of the $P_g(r,t)$, i.e., $F_s(k,t)=\exp[-k^2W(t)]$.

Figure 8 shows the results for $F(k,t)$ vs k, at different times, for a system with $\phi_a=0.38$. $F(k,0)=S(k)$ is the effective 2D static structure factor, the wave vector space analog of $g(r)$. For this particle concentration, $S(k)$ is a highly structured function of the wave vector k, exhibiting several well defined maxima and minima. For $t>0$, the curve of $F(k,t)$ vs k decreases with time and the decay rate is increasingly faster for larger values of the wave vector. Furthermore, the initial decay of $F(k,t)$ vs t is exponential, as it is shown below. Thus, the overall behavior of $F(k,t)$, shown in Fig. 8, is qualitatively similar to the general behavior of the dynamic structure factor of homogeneous 3D systems. Thus, in analogy to Eq. (3.7), we define here the effective 2D hydrodynamic function $H(k)$ as the initial slope of the function $f(k,t)=-k^{-2}S(k)\ln[F(k,t)/S(k)]$. Figure 9 shows $f(k,t)$ vs t, for the system in Fig. 8, for various values of k. As it is seen here, the initial time-evolution of $f(k,t)$ is indeed linear [i.e., the initial decay of $F(k,t)$ is exponential] for a wide range of values of k. Then, we use the initial k-dependent slope of $f(k,t)$ to define $H(k)$. Figure 10 shows $H(k)/D_s^s$, i.e., the effective hydrodynamic function normalized with the initial slope of $W(t)$, for four values of ϕ_a. The structure of $H(k)$ shows that the HI contribute differently to the relaxation of the particle fluctuations of different wavelengths, and that the effect is larger for higher concentrations. One can also see here that single particle motion, characterized by D_s^s (which depends only on ϕ_a but not on k), serves as a reference to the collective motion described by $H(k)$, and that in the limit of large k $H(k)\rightarrow D_s^s$. Deviations of $H(k)$ from D_s^s are due to the fact that collective motion is not just a superposition of the individual motion of the particles, except at values of k where $H(k)=D_s^s$. Although in our case the HI between particles are combined with the hydrodynamic effects from the walls, it is interesting to see that the effective $H(k)$ measured in our systems resembles the hydrodynamic function $H(k)$ measured in 3D suspensions of hard spheres [16]. Although there is not a simple correspondence between quasi-two-dimensional and 3D systems, this observation suggests that, perhaps, the main effect from the walls can be accounted for by the value of D_s^s [the large-k limit of $H(k)$].

E. Self-diffusion versus collective diffusion

Dynamic light scattering (DLS) experiments in 3D suspensions measure the corresponding (3D) $F(k,t)$, i.e., the 3D collective dynamics of the particles. Self-diffusion dynamics is obtained only at large wave vectors where $F(k,t)=F_s(k,t)$. The distinct part of $F(k,t)$ vanishes in this limit, since it is the configuration average of a phase factor that oscillates very rapidly with k. However, at large values of k the correlation function decays very fast, and only the short-time regime of $F_s(k,t)$ is obtained by DLS. Thus, in order to have access to self-diffusion dynamics at larger times [i.e., to $F_s(k,t)$ at lower k], one has to resort to the assumption that $F(k,t)=F_s(k,t)$ at values of $k=k_i$ where $S(k_i)=1$. This assumption is actually equivalent to the assumption that $F_d(k_i,t)=0$. As discussed in Sec. III D, an important advantage of our experiments is that we can determine the self-part and the distinct part of the effective 2D correlation functions independently in the real space. Then, we can determine the self- and distinct-correlation functions in the reciprocal space in the whole range of wave vectors. Thus, we can quantify the relative contributions of $F_s(k,t)$ and $F_d(k,t)$ to the total correlation function $F(k,t)$ for any value of k, particularly for $k=k_i$. As discussed above, the self-part is $F_s(k,t)=\exp[-k^2W(t)]$. Thus, let us show the results for the distinct part. Figure 11 shows the effective 2D $F_d(k,t)$ vs k, at different times, measured in the system with $\phi_a=0.38$. One can appreciate here the time and wavelength dependence of the correlation function between different particles (dots with lines). One can also see here that the distinct part of $F(k,t)$ decays faster for larger values of k and it vanishes in the

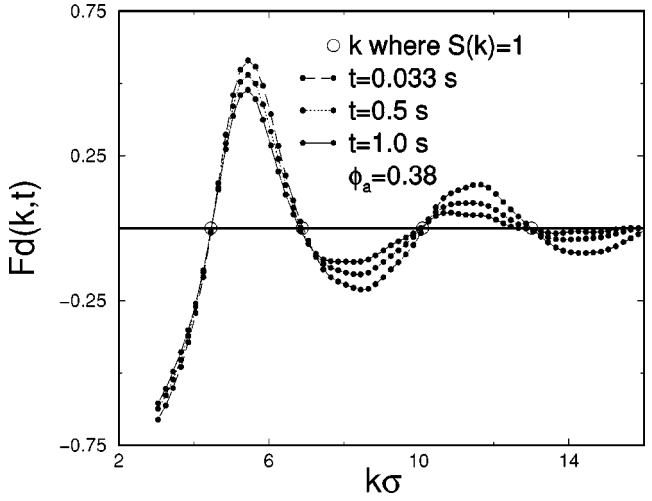

FIG. 11. Time correlation function between different particles $F_d(k,t)$ vs k at different times (dots with lines). Open circles are the values k_i of the wave vector where $S(k)=1$. One can see here that $F_d(k_i,t)=0$ for $t \geqslant 0$.

large wave-vector limit [the behavior of $F_d(k,t)$ is similar to its 3D counterpart]. The open circles represent the values k_i where $S(k_i)=1$. This figure shows that $F_d(k_i,t)$ is vanishing small in the neighborhood of $k=k_i$. Thus, in our quasi-two-dimensional systems one can conclude that $F(k_i,t)=F_s(k_i,t)$. This is an important result that can be useful concerning measurements by light scattering techniques in 3D systems, i.e., it provides experimental support for the assumption that one can measure self-diffusion at wave vectors where the static structure factor equals 1.

IV. CONCLUSIONS

The dynamic properties of colloidal particles confined between two parallel walls was studied by digital video microscopy. The particles form a single layer between the walls, and execute essentially a 2D motion. However, the suspending fluid is not restricted to move only along the plane of motion of the particles; it flows in all directions, coupling (hydrodynamically) the particles motion to the walls. Thus, the system is not 2D, but quasi-2D. The particles dynamics is described in terms of quantities, $G(r,t)$, $F(k,t)$, and their self-components and distinct components, defined and measured here as if the systems were strictly 2D, but which are in reality quasi-2D. We found that these quantities behave in a very similar way as their 3D counterparts. We also report measurements of an effective quantity describing the effects of the hydrodynamic interactions (particle-particle and particle-walls) in quasi-two-dimensional geometries, namely, the effective hydrodynamic function $H(k)$, defined by the initial slope of the effective $F(k,t)$. Interestingly, the quantity $H(k)$ measured here exhibits the same general features of the hydrodynamic function of 3D suspensions of hard spheres. In summary, the results reported here are an important step in understanding the dynamic properties of confined colloidal particles and in particular the role of the HI in restricted geometries, and can serve as a guide for theoretical and computer simulation studies of these phenomena. As an additional result, we show that in our systems the particle fluctuations relax only by self-diffusion at wave vectors where $S(k)=1$. This result is important for the interpretation of measurements of colloidal dynamics by light scattering techniques.

ACKNOWLEDGMENTS

This work was partially supported by the Consejo Nacional de Ciencia y Tecnología (CONACyT, México), Grant Nos. G29589E and ER026 Materiales Biomoleculares, and by Instituto Mexicano del Petróleo, Grant No. FIES-98-101-I.

[1] N. A. Frej and D. C. Prieve, J. Chem. Phys. **98**, 7552 (1993).
[2] L. P. Faucheux and A. J. Libchaber, Phys. Rev. E **49**, 5158 (1994).
[3] M.D. Carbajal-Tinoco, G. Cruz de León, and J. L. Arauz-Lara, Phys. Rev. E **56**, 6962 (1997).
[4] K. Zahn, J. M. Méndez-Alcaraz, and G. Maret, Phys. Rev. Lett. **79**, 175 (1997).
[5] H. Acuña-Campa, M. D. Carbajal-Tinoco, J. L. Arauz-Lara, and M. Medina-Noyola, Phys. Rev. Lett. **80**, 5802 (1998).
[6] A. H. Marcus, J. Schofield, and S. A. Rice, Phys. Rev. E **60**, 5725 (1999).
[7] E. R. Dufresne, T. M. Squires, M. P. Brenner, and D. G. Grier, Phys. Rev. Lett. **85**, 3317 (2000).
[8] T. M. Squires and M. P. Brenner, Phys. Rev. Lett. **85**, 4976 (2000).
[9] R. Pesché and G. Nägele, Phys. Rev. E **62**, 5432 (2000).
[10] J. Santana-Solano and J. L. Arauz-Lara, Phys. Rev. Lett. **87**, 038302 (2001).
[11] P. N. Pusey, in *Liquids, Freezing and Glass Transition*, edited by J. P. Hansen, D. Levesque, and J. Zinn-Justin (Elsevier, Amsterdam, 1991), p. 763.
[12] J. F. Brady, Curr. Opin. Colloid Interface Sci. **1**, 472 (1996).
[13] G. Nägele, Phys. Rep. **272**, 215 (1996).
[14] C. W. J. Beenakker and P. Mazur, Physica A **126**, 349 (1984).
[15] M. Medina-Noyola, Phys. Rev. Lett. **60**, 2705 (1988).
[16] P. N. Segrè, O. P. Behrend, and P. N. Pusey, Phys. Rev. E **52**, 5070 (1995).
[17] A. J. C. Ladd, H. Gang, J. X. Zhu, and D. A. Weitz, Phys. Rev. Lett. **74**, 318 (1995).
[18] W. B. Russel, D. A. Saville, and W. R. Schowalter, *Colloidal Dispersions* (Cambridge University Press, Cambridge, 1989).
[19] G. S. Perkins and R. B. Jones, Physica A **189**, 447 (1992).
[20] L. Lobry and N. Ostrowsky, Phys. Rev. B **53**, 12050 (1996).
[21] J. C. Crocker and D. G. Grier, J. Colloid Interface Sci. **179**, 298 (1996).
[22] D. A. McQuarrie, *Statistical Mechanics* (Harper and Row, New York, 1976).
[23] W. van Megen and S. M. Underwood, J. Chem. Phys. **88**, 7841 (1988).